01 Jul 1999

Fluid Dynamic Parameters in Bubble Columns with Internals

Jinwen Chen

Fan Li

Sujatha Degaleesan

Puneet Gupta

et. al. For a complete list of authors, see https://scholarsmine.mst.edu/che_bioeng_facwork/1374

Recommended Citation

J. Chen et al., "Fluid Dynamic Parameters in Bubble Columns with Internals," *Chemical Engineering Science*, vol. 54, no. 13 thru 14, pp. 2187 - 2197, Elsevier, Jul 1999.
The definitive version is available at https://doi.org/10.1016/S0009-2509(99)00003-2

PERGAMON

Chemical Engineering Science 54 (1999) 2187–2197

Chemical Engineering Science

Fluid dynamic parameters in bubble columns with internals

Jinwen Chen[a], Fan Li[a], Sujatha Degaleesan[a,1], Puneet Gupta[a], Muthanna H. Al-Dahhan[a,*], Milorad P. Duduković[a], Bernard A. Toseland[b]

[a] *Chemical Reaction Engineering Laboratory, School of Engineering and Applied Science, Washington University in St. Louis, One Brookings Drive, Campus Box 1198, St. Louis, MO 63130-3899, USA*

[b] *Air Products & Chemicals, Inc., PO Box 25780, Lehigh Valley, PA 18007, USA*

Abstract

The knowledge of gas holdup, liquid recirculation and turbulent parameters is important for design and performance calculation of bubble column reactors. Although numerous experimental studies have been reported on this subject, most are point measurements limited to columns without internals operated at low gas velocities. In this study, we present the results obtained for the gas holdup profiles, time-averaged liquid velocity profiles, turbulent stresses and eddy diffusivities (radial and axial) obtained in a 18″ (44 cm) diameter column without and with internals similar to those used in industrial scale units (e.g., heat exchanger tubes) using both air/water and air/drakeoil 10 (viscosity ~30 cP) at gas superficial velocities of 2, 5 and 10 cm/s. The scale-up procedure suggested by Degaleesan (1997) is critically examined in light of these results.

Keywords: Bubble column; CARPT; CT; Internals; Turbulent parameters; Eddy diffusivities

1. Introduction

Hydrodynamic properties of bubble/slurry bubble columns play a significant role in chemical and biochemical processes, e.g., Fisher–Tropsch synthesis and waste water treatment. The knowledge of local gas holdup distribution, liquid recirculation velocities and turbulent parameters is important for the design and performance simulation of bubble/slurry bubble column reactors (Deckwer et al., 1987; Fan, 1989, Duduković et al., 1997). Many experimental studies have been reported on this subject in recent years (Chen and Fan, 1992; Menzel et al., 1990; Franz et al., 1984; Groen et al., 1996; Mudde et al., 1997; Devanathan et al., 1990; Kumar et al., 1997; Degaleesan, 1997). However, most of the studies were limited to measurements at several single points or in a small part of the column. Only recently, the Computer Automat Radioactive Particle Tracking (CARPT) and Computed Tomography (CT) techniques, implemented in the Chemical Reaction Engineering Laboratory (CREL), made it possible to measure the time-averaged flow patterns (Devanathan, 1991; Devanathan et al., 1990; Moslemian et al., 1992; Yang et al., 1993), the cross-sectional gas holdup (Kumar, 1994, Kumar et al., 1995, 1997) as well as the turbulent parameters (Degaleesan, 1997, Degaleesan et al., 1997). However, all previous CARPT and CT studies were limited to small columns using air–water, and to columns without internals. Very few studies have been reported for large diameter bubble columns and for liquids more viscous than water. Moreover, time-averaged flow pattern parameters in bubble columns with internals, similar to those used in industrial scale units (e.g., heat exchanger tubes), have not been reported in the open literature.

The objectives of this work are: (1) to obtain the first data for liquid recirculation and turbulent parameters in the full flow field and gas holdup distribution in a 18″ diameter bubble column by using CARPT and CT, (2) to assess the effect of gas superficial velocity and liquid properties on the measured parameters, (3) to quantitatively assess the effect of column internals, and (4) to examine the usefulness of the developed scale-up procedure (Degaleesan, 1997). Finding the flow pattern in the

* Corresponding author. Tel.: 001-314-935-7187; fax: 001-314-935-4832.

E-mail address: muthanna@wuche.wustl.edu (H. Al-Dahhan).

[1] Currently in Shell Oil Company.

0009-2509/99/$ – see front matter
PII: S0009-2509(99)00003-2

18″ column with internals is of particular interest since the same diameter column with such internals is used in commercial practice of the DOE owned, Air Products operated, Alternate Fuels Development Unit (AFDU) in La Porte, Texas.

2. Experimental setup and conditions

2.1. Bubble column setup and operating conditions

In this study, gas holdup, liquid recirculation velocities and turbulent parameters were measured in an 18″ diameter bubble column for air–water system without internals and for air–drakeoil (Drakeoil® 10, Van Waters & Rogers Inc.) with and without internals. The experimental setup is shown in Fig. 1. The column is made of Plexiglas with a diameter of 18 in (44 cm of inner diameter) and a height of 8 ft. The distributor used is a perforated plate with the hole diameter of 0.77 mm and an open area of 0.076% (301 holes distributed on 14 concentric circular rings which are 1.5 cm apart). The internals are composed of two bundles of 1″ aluminum tubes (1/16″ in thickness) which are located at two different radial positions, namely, at dimensionless radius, r/R, of 0.39 and 0.61, respectively. Each bundle contains 8 equally distributed tubes as illustrated in Fig. 2. These internals were designed so as to simulate the heat exchanger tubes in the slurry bubble column AFDU reactor for methanol synthesis in La Porte, Texas.

For comparison, CARPT and CT experiments were conducted at the superficial gas velocities of 2, 5, and 10 cm/s for the air–water system without internals, and the air–drakeoil system with and without internals. The liquid was in batch mode with a static height of about 170 cm. CT scans were performed for each superficial gas velocity at four axial elevations, 51, 89, 132 and 170 cm from the distributor.

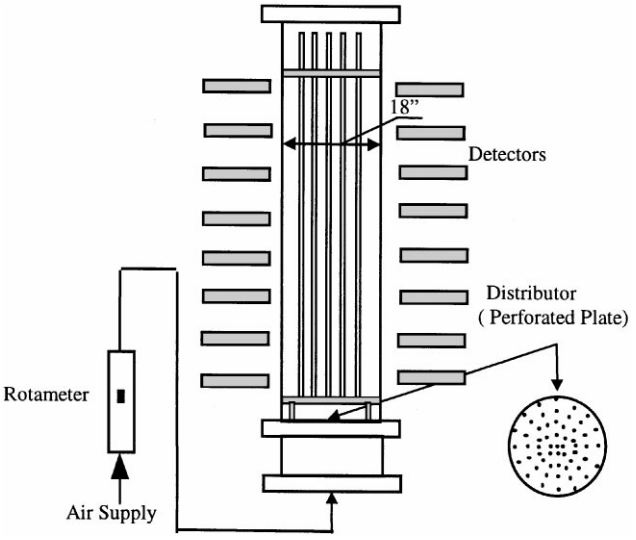

Fig. 1. Experimental setup for the 18″ diameter bubble column.

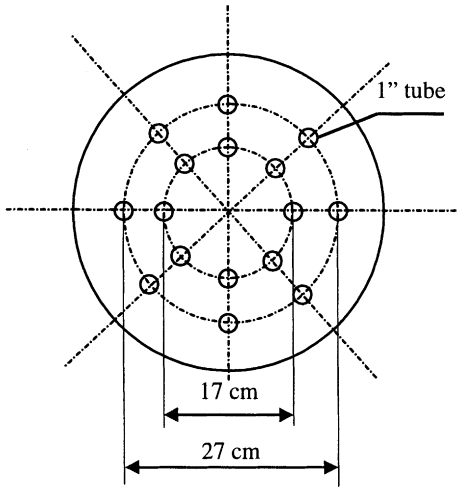

Fig. 2. Configuration of the internals.

2.2. CT facility

The details of the scanner hardware and software used in CREL are described elsewhere (Kumar, 1994; Kumar et al., 1995, 1997). Basically the scanner consists of an array of NaI (Tl) detectors of 5 cm in diameter) (11 detectors were used for the present study) and an encapsulated Cesium-137 (Cs^{137}) source (100 mCi) located opposite to the center of the array of the detectors. The detectors and the source are mounted on a plate, which can be rotated around the axis of the column by a step motor. Moreover, the whole assembly can be moved up and down along the column to scan different axial elevations of the column. The source collimator provides a fan beam of 40° in an horizontal plane. There are rectangular holes (0.5 cm × 1.0 cm) on the detector collimator at locations corresponding to each of the detectors for sampling the gamma-ray beams. The dimensions of the collimator were optimized based on the consideration of providing adequate area for detecting photons with good statistics at the chosen sampling frequency (Kumar, 1994). This design of the CT scanner yields a spatial resolution of 0.35 and 1 cm in horizontal and vertical directions, respectively. By an inversion process of the measured projections, time-averaged gas holdup distribution in the cross section of the column can be reconstructed with a proper reconstruction algorithm. In this work, the Estimation–Maximization (EM) algorithm is used for image reconstruction, the details of which are provided elsewhere (Kumar, 1994). Due to the limitation of the design of the current CT scanner in CREL, phase holdup distribution can be obtained only as a time-averaged one in two-phase flow system.

2.3. CARPT facility

As a non-invasive method, CARPT has been proven to be a powerful technique to study flow patterns in multiphase flow systems. It can monitor liquid motion in bubble columns (Devanathan et al., 1990; Moslemian et al., 1992; Yang et al., 1993; Degaleesan et al., 1997), solids motion in gas–solid fluidized bed (Lin et al., 1985; Moslemian et al., 1992), solid motion in liquid–solids and gas–liquid–solids fluidized beds (Limtrakul, 1996) and in liquid–solid risers (Roy et al., 1997). Details about the software and hardware can be found elsewhere (Devanathan, 1991). In this study, 5 radioactive Scandium-46 (Sc^{46}) particles emitting gamma rays of constant energy of 0.89 and 1.12 MeV were embedded into a polypropylene particle with a diameter of about 2.38 mm. The density of the particle (scandium + polypropylene) was made equal to the density of the liquid phase being tracked. Two such particles were made, one to match the density of water ($\rho_l = 1.0$ g/cm^3) and the other to match the density of drakeoil ($\rho_l = 0.86$ g/cm^3). Upon irradiation the particle activity was 400 μCi. The intensity of the gamma rays emitted by the tracer particle is continuously monitored by an array of 30 NaI (Tl) scintillation detectors (5 cm in diameter) which are strategically located around the column. Calibrations are performed prior to the experiments for each detector to determine the particle position at each instant in time. An instantaneous velocity is calculated by time differentiation and assigned to a cell that contains the mean particle position between two successive locations. The instantaneous velocities are then averaged in each cell, over the whole time span of the CARPT experiments, to get time-averaged particle velocities. Ensemble averaged, or time averaged by the ergodic hypothesis, velocities and other turbulence quantities can be calculated for all column locations upon running the experiment for many hours (over 40 h in this study). The sampling frequency of the system can be as high as 500 Hz. However, due to the limitation in radioactive particle strength and the inertia of the particle, 50 Hz is normally used in CARPT experiments and thus flow events with frequency up to 25 Hz can be captured.

3. Results and discussions

3.1. Gas holdup obtained by CT scans

The reconstructed CT image, processed from data obtained through CT scans, provides the time-averaged cross-sectional gas holdup distribution. Radial gas holdup profiles are obtained by azimuthal averaging at a given axial level. Fig. 3a–c exhibits the cross-sectional gas holdup distribution for the systems of air–water, air–drakeoil without internals and air–drakeoil with

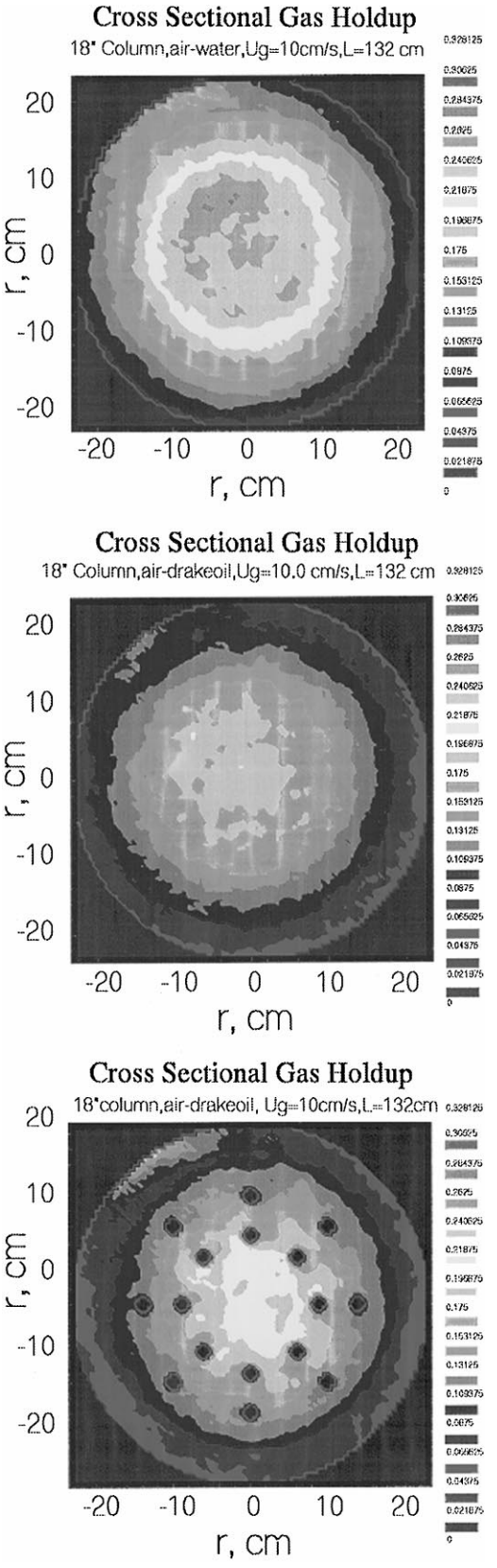

Fig. 3. Cross-sectional gas holdup distribution, $U_g = 10$ cm/s: (a) air–water without internals; (b) air–drakeoil without internals; and (c) air–drakeoil with internals.

internal at gas superficial velocity of 10 cm/s. The gas holdup is high in the center and low near the wall of the column as seen from the images. This kind of distribution in bubble columns is in line with the results obtained by CT scans in smaller diameter bubble columns (Kumar, 1994, Kumar et al., 1995, 1997) and is confirmed by using different measuring methods (Menzel et al., 1990; Franz et al., 1984; Goren et al., 1996, Hebrard et al., 1996). In Fig. 3a, the bright spots represent the shape and position of the internal tubes. It is evident from these figures that the cross-sectional gas holdup distribution is almost axi-symmetric at high gas superficial velocities. However, this is not the case at low gas superficial velocities where much more distinct asymmetry is observed. The possible reasons for this have been discussed elsewhere (Chen et al., 1998).

Radial gas holdup profiles can be obtained by azimuthally averaging the cross-sectional gas holdup distribution. Fig. 4 shows the radial gas holdup profiles at different superficial gas velocities for the air–drakeoil system, while Fig. 5 illustrates the radial gas holdup profiles for the three systems studied at gas superficial velocity of 10 cm/s. Gas holdup increases with the increase in gas superficial velocity as illustrated in Fig. 4. Due to the large bubbles formed in drakeoil, which is much more viscous than water, gas holdup in the air–drakeoil system (without internals) is lower than that in the air–water system. Gas holdup in air–drakeoil system with internals is slightly higher than that in the system without internals as seen in Fig. 5. However, the difference is not significant, indicating that the presence of internals does not affect much the overall flow pattern in the column for the range of employed superficial gas velocities. This is verified by CARPT experiments and is discussed in the next section.

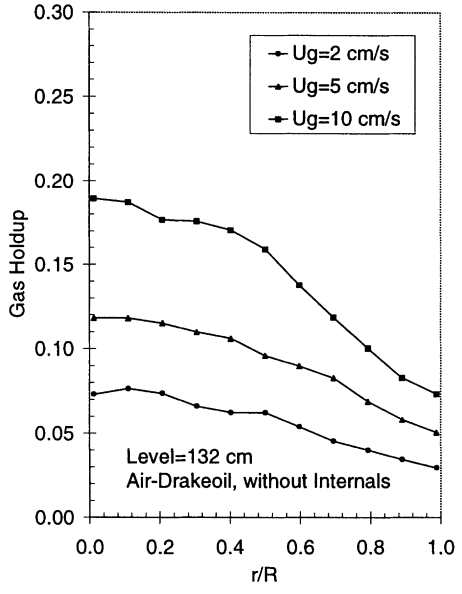

Fig. 4. Gas holdup at different gas superficial velocities, level = 132 cm, air–drakeoil system without internals.

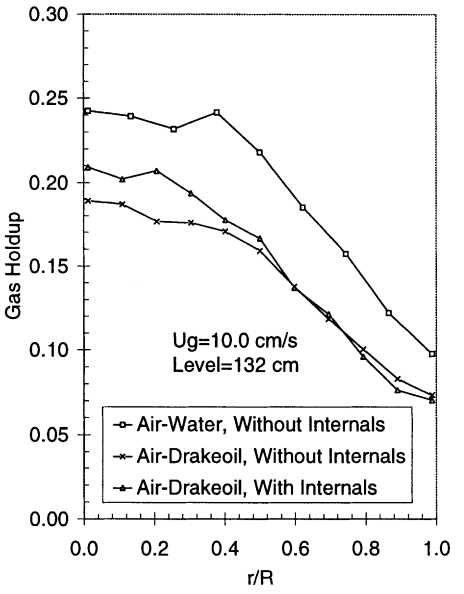

Fig. 5. Comparison of gas holdup for different systems, $U_g = 10$ cm/s, level = 132 cm.

3.2. Liquid recirculation velocity and turbulent stresses

As discussed above, gas holdup in a bubble column is high in the center and low at the wall and this leads to a gross liquid circulation throughout the column with liquid flowing up in the center and down near the wall. Fig. 6 displays the side view of the two-dimensional time-averaged velocity vector plot at gas superficial velocity of 10 cm/s for the air–drakeoil system. The gross flow pattern is evident from the plot and is axisymmetric due to the symmetric distribution of gas holdup. Similar observation can be made for the air–water and air–drakeoil system with internals. From the plot one can also see that the flow in the bottom part of the column seems not developed well, indicating strong entrance effect for a highly viscous system like air–drakeoil.

Note that all liquid velocities and other turbulent quantities obtained by CARPT are three dimensional. By azimuthal averaging, one can get radial profiles of these quantities. Fig. 7a and b shows the comparison of the radial profiles of the time-averaged axial liquid velocities obtained for the air–water system without internals, and air–drakeoil with and without internals at gas superficial velocity of 10 cm/s. These velocities are obtained by averaging only over the developed flow region of the column. It is clear that in the time-averaged sense the liquid flows up in the center and flows down near the wall. This kind of flow pattern has been reported by many investigators in bubble columns (Devanathan et al., 1990; Chen et al., 1994; Menzel et al., 1990; Franz et al., 1984; Mudde et al., 1997) in airlift loop reactors (Young et al., 1991), in gas–solid fluidized beds

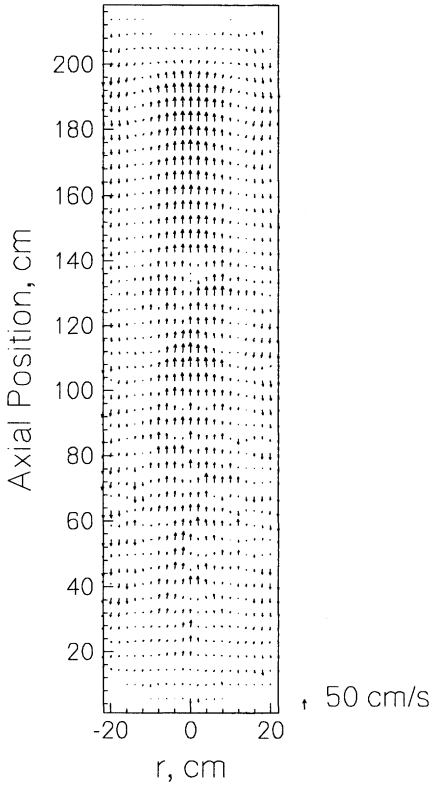

Fig. 6. Two-dimensional vector plot, air–drakeoil system without internals, $U_g = 10.0$ cm/s.

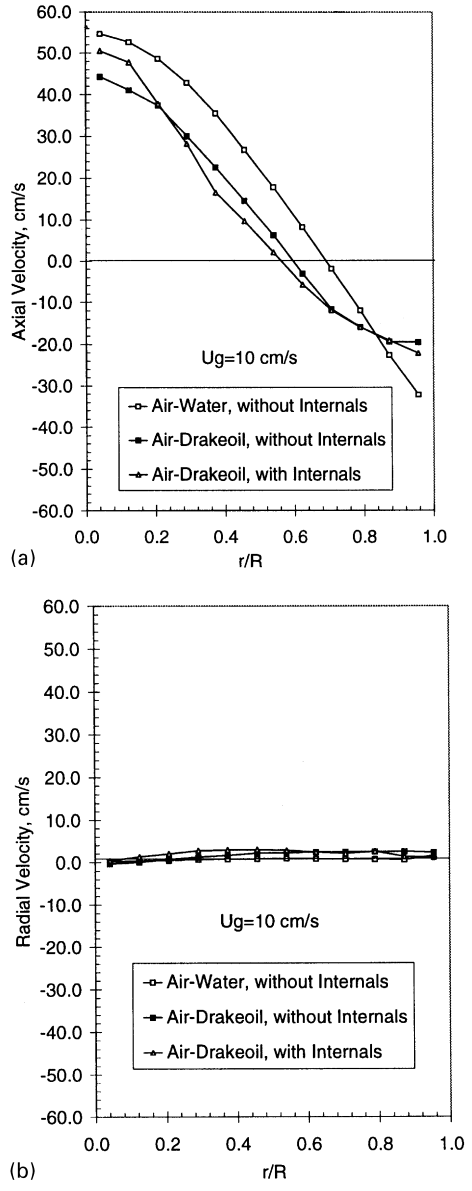

Fig. 7. Time-averaged liquid recirculation velocities: (a) axial velocity and (b) radial velocity.

(Moslemian et al., 1992), in liquid–solid and gas–liquid–solid fluidized beds (Limtrakul, 1996). The axial velocity inversion point is at dimensionless radius, r/R, of 0.68 for the air–water system. The inversion point moves radially towards the center of the column for the air–drakeoil system without internals and even further for air–drakeoil with internals, 0.60 and 0.57 respectively. Compared with the ensemble-averaged axial velocities, the ensemble-averaged radial velocities are very low fluctuating around zero, as shown in Fig. 7b. The maximum time-averaged radial velocity measured in the column for the air–drakeoil system with internals is about 3 cm/s. In the first approximation, it can be accepted that the time-averaged liquid radial velocity is zero in the developed region of flow for these systems studied.

The knowledge and understanding of liquid turbulence are very important in modeling gas–liquid flows in bubble columns (Jakobsen et al., 1996). The turbulent interactions between the large eddies observed in the column can be characterized by the auto/cross correlations of fluctuating quantity components (Degaleesan, 1997). The secondary order velocity correlations, $u_i' u_j'$, represent the momentum transport effect along the ith direction due to the instantaneous flow in the jth direction. Thus the turbulent stress tensors, or Reynolds stresses, can be defined by the following symmetric matrix in a cylindrical coordinate system:

$$\tau = \begin{bmatrix} \overline{u_r' u_r'} & \overline{u_r' u_\theta'} & \overline{u_r' u_z'} \\ \overline{u_\theta' u_r'} & \overline{u_\theta' u_\theta'} & \overline{u_\theta' u_z'} \\ \overline{u_z' u_r'} & \overline{u_z' u_\theta'} & \overline{u_z' u_z'} \end{bmatrix}, \quad (1)$$

where $\overline{u_i' u_j'} = \overline{u_j' u_i'}$. The traditional Reynolds stress is defined as $-\rho_l \overline{u_j' u_i'}$. Since the main emphasis of the present work is on experimental measurements and understanding the mechanisms of turbulence, and since the density of the liquid is constant, the negative sign and the liquid density term are not taken into account in this study.

By CARPT measurements, it is possible to estimate all the above quantities in the entire flow field of the column.

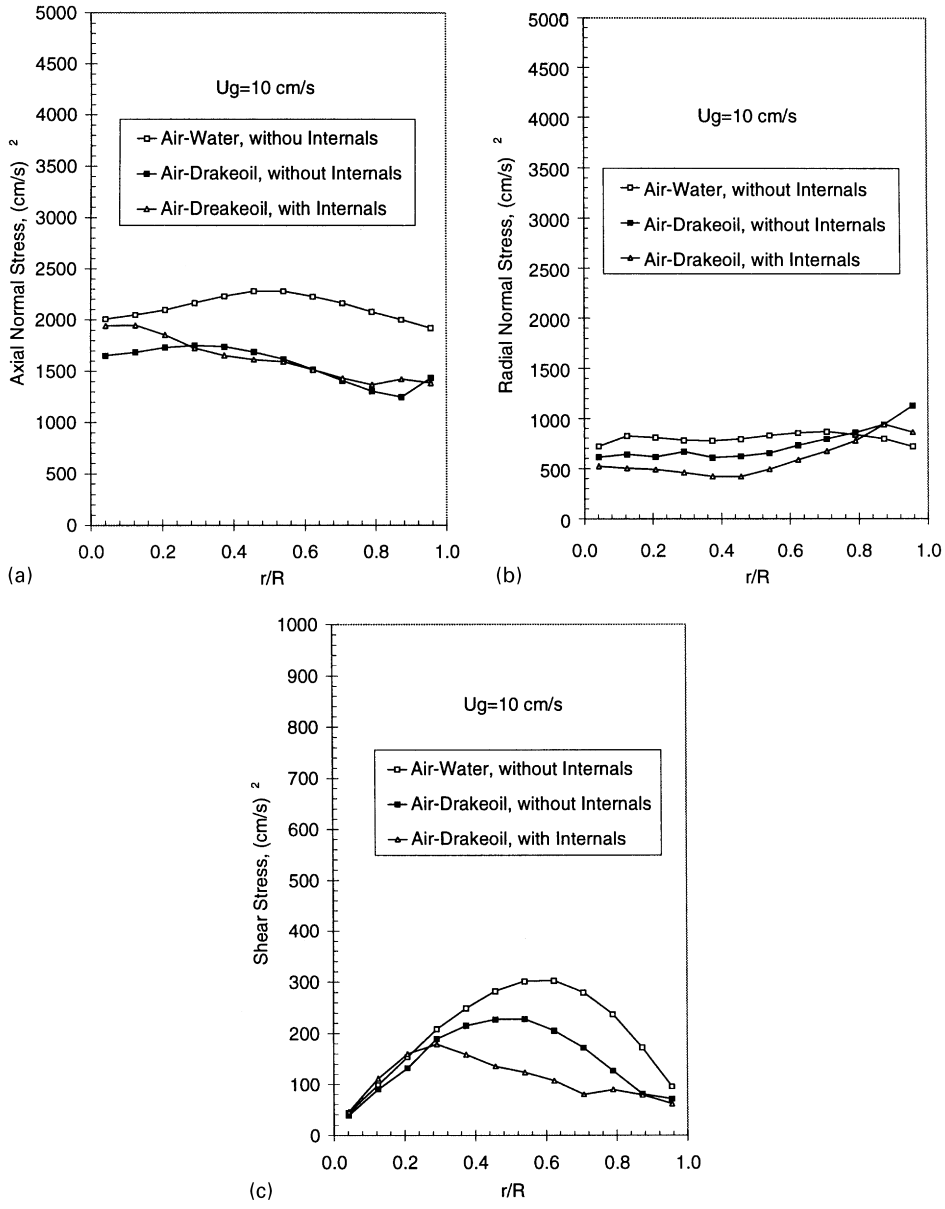

Fig. 8. Turbulent stresses for different systems, $U_g = 10$ cm/s: (a) axial normal stress; (b) radial normal stress; and (c) shear stress.

However, since the effects of the entrance and the outlet on flow are significant in this study, only the developed flow regions are considered when axially averaging these quantities. Moreover, only the axial and radial normal stresses and the shear stress are presented in this paper since they are most frequently used in two-dimensional modeling of bubble columns.

As seen in Fig. 8a the normal stress in the air–water system is always higher than in the air–drakeoil systems with a maximum value at dimensionless radius of 0.5. The magnitude and the radial profile of the normal stresses in the systems with and without internals are almost the same with small differences in the center and near the wall of the column. The radial normal stresses for the three systems show the same trends with relatively flat profile as shown in Fig. 8b. Similarly to the axial normal stress, the magnitude of the radial normal stress in the air–drakeoil system without internals is lower than in the air–water system (without internals), indicating that the increased viscosity of drakeoil reduces the turbulence in the column. The radial normal stress is higher in the air–drakeoil system without internals than in the one with internals, which is understandable since the presence of the internals physically reduces the mixing scale in the radial direction. As to the shear stresses, similar trend in its profile is evident in Fig. 8c. Maximum in the value of the shear stress is observed for all the three systems while the shear stress is close to zero in the center and near the wall of the column. The radial locations of the maximum value seem to be related to the axial

velocity inversion point. However, for the air–drakeoil system with internals, the radial location of the maximum shear stress value moves further to the center of the column compared with axial velocity inversion point for the same system. In summary, the increased viscosity of drakeoil reduces the gas holdup distribution and thus reduces the liquid recirculation velocity and turbulent stresses, while the presence of the internals affects somewhat the flow patterns and turbulence in the column. However, the differences between the column with and without internals are not large.

3.3. Turbulent eddy diffusivities

Normally, the eddy diffusivity that appears in the governing equations of bubble column models is arbitrarily assigned or further modeled. Experimental evaluation of this important parameter is needed. The turbulent eddy diffusivities defined in this work are based on the Lagrangian frame-work due to the nature of CARPT data, and can be represented by the following equation (Degaleesan, 1997):

$$D_{ij}(t) = \frac{1}{2}\frac{\mathrm{d}}{\mathrm{d}t}\overline{y_i y_j} = \frac{1}{2}(\overline{u_i' y_j} + \overline{u_j' y_i}), \quad i = 1\text{–}3,\ j = 1\text{–}3, \tag{2}$$

where u_i' is the fluctuating velocity in i-direction, and y_i is displacement of fluid due to fluctuating Lagrangian velocity in the i-direction.

In a bubble column, the flow is anisotropic, and the radial gradient of the time-averaged liquid axial velocity has to be considered in the evaluation of axial eddy diffusivities. Moreover, according to experimental results, the other velocity derivatives are almost zero and are not considered in the computation. In other words:

$$\frac{\partial u_z}{\partial r} \neq 0 \quad \frac{\partial u_z}{\partial \theta} = \frac{\partial u_r}{\partial z} = \frac{\partial u_f}{\partial \theta} = \frac{\partial u_\theta}{\partial r} = \frac{\partial u_\theta}{\partial z} = 0. \tag{3}$$

Thus the displacements in all the three directions are obtained as follows (Degaleesan, 1997):

$$y_r(t) = \int_0^t u_r'(t')\,\mathrm{d}t', \tag{4}$$

$$y_\theta(t) = \int_0^t u_\theta'(t')\,\mathrm{d}t', \tag{5}$$

$$y_z(t) = \int_0^t \left(\left(\frac{\mathrm{d}u_z}{\mathrm{d}r}\right)\bigg|_{y_r(t')} y_r(t') + u_z'(t')\right)\mathrm{d}t'. \tag{6}$$

In Eq. (6), the term $(\mathrm{d}u_z/\mathrm{d}t)|_{y_r(t')}\, y_r(t')$ is introduced to consider the effect of the mean axial velocity gradient in the radial direction. Using the definition of the turbulent eddy diffusivities, D_{ij}, given by Eq. (2), the eddy diffusivities in radial, azimuthal and axial directions are calculated as

$$D_{rr}(t) = \frac{1}{2}\frac{\mathrm{d}}{\mathrm{d}t}\overline{y_r^2(t)} = \int_0^t \overline{u_r'(t')u_r'(\tau)}\,\mathrm{d}\tau, \tag{7}$$

$$D_{\theta\theta}(t) = \frac{1}{2}\frac{\mathrm{d}}{\mathrm{d}t}\overline{y_\theta^2(t)} = \int_0^t \overline{u_\theta'(t')u_\theta'(\tau)}\,\mathrm{d}\tau, \tag{8}$$

$$D_{zz}(t) = \frac{1}{2}\frac{\mathrm{d}}{\mathrm{d}t}\overline{y_z^2(t)} = \overline{y_z(t)u_z'(t)} = \int_0^t \left\{\overline{\left.\frac{\partial u_z}{\partial r}\right|_{y_r(t')}\left(\int_0^{t'} u_z'(t)u_r'(\tau)\,\mathrm{d}\tau\right)} + \overline{u_z'(t)u_z'(t')}\right\}\mathrm{d}t'. \tag{9}$$

From Eqs. (7)–(9), it is evident that the calculation of the eddy diffusivities is related to the Lagrangian auto-correlation coefficients and cross-correlation coefficient. The evaluation of Lagrangian correlation coefficients form CARPT data is described by Degaleesan (1997) and is not presented here. Since the eddy diffusivities are functions of position as well as time, only the asymptotic values are considered as representatives for the axial and azimuthal eddy diffusivities and only the axial and radial eddies, which are most of interest, are presented in this paper.

As shown in Fig. 9a, at gas superficial velocity of 10 cm/s, the axial eddy diffusivities in the air–water system (without internals) are similar to that in the air–drakeoil system (without internals) from the center of the column to dimensionless radius, r/R, of 0.6. However, axial eddy diffusivities in air–water are higher in the region from $r/R = 0.6$ to the wall of the column. The axial eddy diffusivities in the air–drakeoil system with internals are somewhat lower than those in the system without internals (Fig. 9a), indicating some effects of internals on the axial eddy diffusivities. Compared to the axial diffusivities, larger relative differences are observed for the eddy radial diffusivities for the three systems as seen in Fig. 9b. The radial eddy diffusivities in air–water (without internals) are much higher (50% higher) than those in the air–drakeoil system (without internals). This means that the effect of viscosity on turbulent diffusivities is more pronounced in the radial direction. Similarly, one can note that the eddy diffusivity in the air–drakeoil system with internals is lower than in the system without internals (see Fig. 9b), which is expected due to the fact that presence of the internals physically reduces the radial turbulence length scale since the internal tubes restrict the flow in the radial direction. This qualitatively verifies Degaleesan's assumption for the methanol reactor in La Porte, in which internals with similar configuration as used in this study were employed as heat exchangers (Degaleesan, 1997). It should also be noted that the radial locations at which the axial and radial eddy diffusivities exhibit maximum values shift towards the center of the column as one moves from air–water system (without internals) through air–drakeoil system

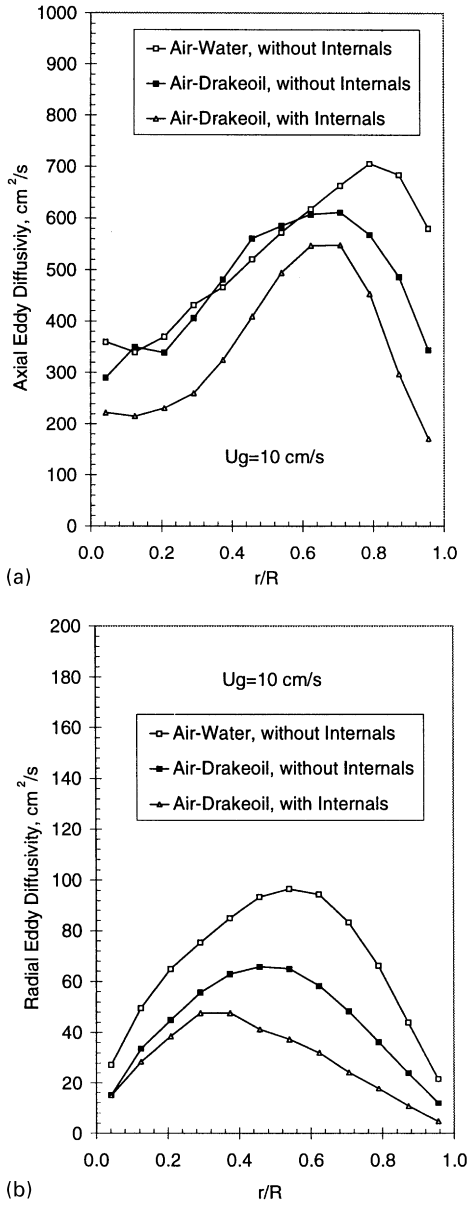

Fig. 9. Comparison of eddy diffusivities, $U_g = 10$ cm/s: (a) axial eddy diffusivities and (b) radial eddy diffusivities.

without internals to air–drakeoil system with internals (Fig. 9). This is similar to what is observed for turbulent shear stresses in Fig. 8c.

3.4. Evaluation of scale-up procedures

Degaleesan (1997) and Degaleesan et al. (1997) presented a procedure to obtain reasonable predictions of liquid–phase tracer data performed in the methanol synthesis slurry bubble column reactor at La Porte, Texas by using the convection–diffusion models for liquid mixing in bubble columns. In the methanol reactor, which is 46 cm (18″) in diameter, two bundles of heat exchanger tubes (1″ in diameter), 12 tubes in each bundle, are fixed along the column at dimensionless radial locations of 0.41 and 0.54, respectively, which is similar to the internals used in this study. Additional details about the reactor can be found elsewhere (Degaleesan, 1997; Degaleesan et al., 1997). However, since no CARPT data were available for the reactor column with internals, the axial liquid recirculation velocity profile was obtained by a one-dimensional recirculation model with radial gas holdup profiles as input. It was also assumed that the heat exchanger tubes have effects only on the radial eddy diffusivities by considering the characteristic spacing between the tubes (Degaleesan, 1997). Evaluation of the above scale-up procedure for the effect of internals can be made based on the experimental data obtained in this study with air–drakeoil systems with and without internals.

3.4.1. Liquid recirculation velocity

A one-dimensional recirculation model was proposed to simulate the liquid flow pattern in bubble columns (Kumar, 1994; Kumar et al., 1994). The details of the model will not be presented in this paper. The model uses radial gas holdup profile and radial mixing length profile as inputs. The radial gas holdup profile can be obtained by fitting the experimental holdup profile data with the equation

$$\varepsilon_g(\xi)\tilde{\varepsilon}\frac{m+2}{m}(1-c\xi^m), \tag{10}$$

where ξ is the dimensionless radial position, m is the exponent, c is the parameter that allows for the possibility of non-zero gas holdup close to the wall and $\tilde{\varepsilon}$ is a parameter related to the cross-sectional mean gas holdup. For the one-dimensional velocity model (Kumar, 1994), the shear stress can be represented as

$$\tau_{rz}(\xi) = \frac{\rho_l g R}{2}\left[\frac{2\tilde{\varepsilon}}{m\lambda^2}\right]\xi c\left(1-\left(\frac{\xi}{\lambda}\right)^m\right], \quad \xi \leqslant \lambda \tag{11}$$

in which ρ_l is the liquid density, λ is the dimensionless radial position of the maximum downward liquid velocity. The mixing length profile can then be evaluated by the representation of the shear stress with the following equation:

$$\tau_{rz}(\xi) = \frac{\rho_l \upsilon_m}{R}\left(-\frac{\mathrm{d}u_z}{\mathrm{d}\xi}\right) + \rho_l\frac{l^2(\xi)}{R}\left(-\frac{\mathrm{d}u_z}{\mathrm{d}\xi}\right)^2, \quad \xi \leqslant \lambda, \tag{12}$$

where v_m is the kinematic viscosity of the liquid, $\mathrm{d}u_z/\mathrm{d}\xi$ is the radial gradient of the liquid time-averaged recirculation velocity which can be evaluated from CARPT measurements. The mixing length is then fitted with the following empirical correlation:

$$l(\xi) = \frac{a(1-\xi)}{(\xi+b)^f} + d(1-\xi)^e. \tag{13}$$

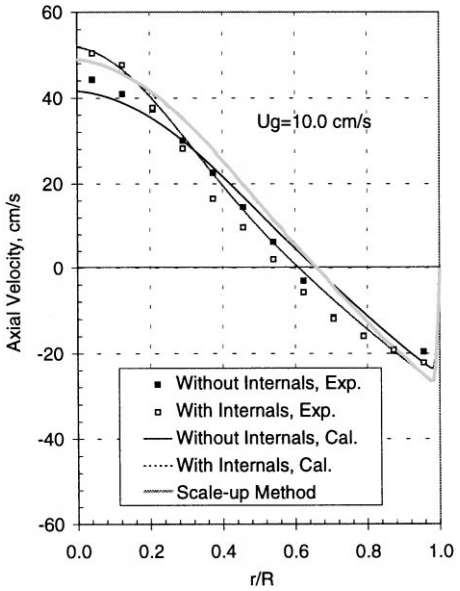

Fig. 10. One-dimensional model simulation of liquid recirculation velocity, $U_g = 10.0$ cm/s.

Using the CT measured gas holdup profile and the mixing length profile obtained from CARPT measured shear stress profile, the radial profile of axial liquid recirculation velocity can be computed from the one-dimensional model.

Fig. 10 shows the computed results as well as the experimentally measured ones for the air–drakeoil systems with and without internals. The computed results are in reasonable agreements with the CARPT measured ones. The computed result based on the scale-up method used by Degaleesan (1997) and Degaleesan et al. (1997) is also plotted in Fig. 10. The calculation is performed by using the gas holdup information obtained in the column with internals and the liquid mixing information in the column without internals, which is similar to the treatment for La Porte slurry bubble column reactor for methanol synthesis (Degaleesan, 1997). It is seen that the simulated result with the scale-up method is slightly higher than one for the air–drakeoil system with internals except in the center of the column. The mean liquid recirculation velocities, $\bar{u}_{\mathrm{rec}}$, or the average liquid inflow, which is defined as

$$\bar{u}_{\mathrm{rec}} = \frac{\int_0^{r^*} u_z(r)\,\varepsilon_l(r)\,r\,\mathrm{d}r}{\int_0^{r^*} \varepsilon_l(r)\,r\,\mathrm{d}r}, \tag{14}$$

where r^* is the radial location of the flow inversion point and $\varepsilon_l(r)$ is the liquid holdup, are 18.8 and 20.2 cm/s for the system with internals and the scale-up method, respectively. The difference, in terms of $\bar{u}_{\mathrm{rec}}$ is 7.4%, which is acceptable for engineering estimations.

3.4.2. The radial eddy diffusivity

In the treatment of the liquid tracer data from the AFDU La Porte facility, Degaleesan et al. (1997) assumed that the radial effective diffusivities are considerably reduced due to the presence of the internals. They were essentially scaled downwards by the ratio of the spacing between internals and column diameter. However, CARPT measurements (Fig. 9b) indicate that such a large reduction in radial eddy diffusivities does not occur. This is partly due to the fact that the area of a cylindrical surface occupied by tubes and, hence, blocked for radial transport is only 37% for the inner bundle of tubes and 23% for the outer bundle. For such internals the reduction in observed radial eddy diffusivities is relatively small (Fig. 9b). This implies that the procedure for estimation of radial eddy diffusivities proposed by Degaleesan (1997) and Degaleesan et al. (1997) will have to be re-examined.

4. Conclusions

1. At high gas velocity (10 cm/s), gas holdup and liquid recirculation flow pattern is axisymmetric in the fully developed flow region of the column for the three systems air–water, air–drakeoil without/with internals investigated in this study.
2. Gas holdup in air–drakeoil is lower than in air–water due to the large bubbles formed in the former system. Gas holdup in the column with internals is slightly higher than in the column without internals.
3. The time-averaged axial velocity in air–water system is higher than in air–drakeoil due to higher gas holdup/radial gas holdup gradient in the former system. The high viscosity of drakeoil not only reduces the liquid recirculation velocity, but also pulls the velocity inversion point inward to the center of the column.
4. There are no significant differences in both the liquid recirculation velocity and the velocity inversion point for the columns with and without internals, indicating that the presence of the internals does not affect the gas liquid recirculation flow pattern for the range of superficial gas velocities studied.
5. At high gas superficial velocity (10 cm/s), the turbulent stresses and eddy diffusivities in air–water (without internals) are higher than in air–drakeoil (without internals). The internals do somewhat affect the turbulent stresses and eddy diffusivities in both radial and axial directions. Turbulent stresses and eddy diffusivities are lower in the column with internals due to the fact that they physically reduce the length scales of turbulence. The difference is more pronounced in the radial direction than in axial direction.
6. The scale-up procedure suggested by Degaleesan (1997) is critically examined in light of the results

obtained in the air–drakeoil systems with and without internals and seems to yield reasonable predictions for liquid recirculation.

Acknowledgements

The authors are indebted to the industrial sponsors of CREL and to Department of Energy under contract to Air-Products, DOE FC 22 95 PC 95051.

Notation

a, b, d, e, f	parameters in Eq. (13)
c	parameters in Eq. (10)
D_{ij}	eddy diffusivity, cm^2s
$D_{rr}, D_{\theta\theta}, D_{zz}$	eddy diffusivities in r, θ, z directions, respectively, cm^2/s
l	mixing length, cm
m	parameter in Eq. (10)
r	radial position, cm
R	radius of column, cm
u_r, u_θ, u_z	velocity vectors in r, θ, z directions, cm/s
u'_r, u'_θ, u'_z	fluctuating velocity vectors in r, θ, z directions, cm/s
$\bar{u}_{rec}$	mean liquid upflow velocity, cm/s
U_g	superficial gas velocity, cm/s
y_r, y_θ, y_z	displacements due to fluctuations in r, θ, z directions, respectively, cm

Greek letters

ε_g	gas holdup
ε_l	liquid holdup
$\tilde{\varepsilon}$	parameter in Eq. (10)
λ	dimensionless radial location of axial velocity inversion point, cm
v_m	kinematic viscosity, cm^2/s
θ	coordinate in angular direction
ρ_l	liquid density, g/cm^3
τ	turbulent stress defined in Eq. (1), cm^2/s^2
τ_{rz}	turbulent shear stress in r and z directions, $g/cm\,s^2$
ξ	dimensionless radial coordinate, r/R

Subscripts

i, j	direction i, j
g	gas phase
l	liquid phase
r	radial coordinate
θ	angular coordinate
z	axial coordinate

Superscripts

$'$	fluctuation quantities

References

Chen, J., Gupta, P., Al-Dahhan, M.H., Duduković, M.P., & Toseland, B.A. (1988). Gas holdup distributions in large diameter bubble columns measured by computed tomography. *Flow Measurement and Instrumentation*, *9*, 91–101.

Deckwer, W.D. (1987). Bubble columns – the state of the air and current trends. *Internatinal Chemical Engineers*, *27*(3), 405–422.

Chen, R.C., & Fan, L.-S. (1992). Particle image velocimetry for characterizing the flow structure in three-dimensional gas–liquid–solid fluidized beds. *Chemical Engineering Science*, *47*(13/14), 3615–3622.

Degaleesan, S. (1997). *Fluid dynamic measurements and modeling of liquid mixing in bubble columns*. Ph.D. Thesis, Washington, University in St. Louis, USA.

Degaleesan, S., Duduković, M.P., Toseland, B.A., & Bhatt, B.L. (1997). A two-compartment convective-diffusion model for slurry column reactors. *Industrial and Engineering Chemistry Research*, *36*(11), 4670–4680.

Devanathan, N. (1991). *Investigation of liquid hydrodynamics in bubble columns via computer automated radioactive particle tracking*. Ph.D. Thesis, Washington University in St. Louis, USA.

Devanathan, N., Moslemian, D., & Duduković, M.P. (1990). Flow mapping in bubble columns using CARPT. *Chemical Engineering Science*, *45*(8), 2285–2291.

Duduković, M.P., Degaleesan, S., Gupta, P., & Kumar, S.B. (1997). Fluid dynamics in Churn-turbulent bubble columns: Measurements and modeling. *Proceedings of the ASME Fluids Engineering Division Summer Meeting*, 244 (3517), Vancouver, Canada (Proceedings available on a CD-ROM).

Fan, L.S. (1989). *Gas–liquid–solid fluidization engineering*. Butterworths Series in Chemical Engineering, Boston, USA.

Franz, K., Borner, T., Kantorek, H.J., & Buchholz, R. (1984). Flow structures in bubble columns. *German Chemical Engineering*, *7*, 365–374.

Groen, J.S., Oldeman, R.G.C., Mudde, R.F., & Van Den Akker, H.E.A. (1996). Coherent structure and axial dispersion in bubble column reactors. *Chemical Engineering Science*, *51*(10), 2511–2520.

Hebrard, G., Bastoul, D., & Roustan, M. (1996). Influence of the gas sparger on the hydrodynamic behaviour of bubble columns. *Transactions of the Institution of Chemical Engineers*, *74* (Part A), 406–414.

Jakobsen, H.A., Sannaes, B.H., Grevskott, S., & Svendsen, H.F. (1996). Modelling of bubbly flows. Presented at *Engineering Foundation Conference on Computational Fluid Dynamics in Chemical Engineering*, San Diego, USA, October 13–18.

Kumar, B.S. (1994). *Computer tomographic measurements of void fraction and modeling of the flow in bubble columns*. Ph.D. Thesis, Florida Atlantic University, USA.

Kumar, B.S., Devanathan, N., Moslemian, D., & Duduković, M.P. (1994). Effect of scale on liquid recirculation in bubble columns. *Chemical Engineering Science*, *49*(24b), 5673–5652.

Kumar, B.S., Moslemian, D., & Duduković, M.P. (1995). A gamma ray tomographic scanner for imaging void fraction distribution in bubble columns. *Flow Measurement and Instrument*, *6*(1), 61–73.

Kumar, S.B., Moslemian, D., & Duduković, M.P. (1997). Gas holdup measurements in bubble columns using computed tomography. *The American Institute of Chemical Engineers Journal*, *43*(6), 1414–1425.

Limtrakul, S. (1996). *Hydrodynamics of liquid fluidized beds and gas–liquid fluidized beds*. Ph.D. Thesis, Washington University in St. Louis, USA.

Lin, J.S., Chen, M., & Chao, B.T. (1985). A novel radioactive particle tracking facility for measurement of solids motion in gas fluidized beds. *The American Institute of Chemical Engineers Journal*, *31*(2), 465–473.

Menzel, T., in der Weide, T., Staudacher, O., Wein, O., & Onken, U. (1990). Reynolds shear stress for modeling of bubble column reactors. *Industrial & Engineering Chemistry Research*, *29*(6), 988–994.

Moslemian, D., Devanathan, N., & Duduković, M.P. (1992). Radioactive particle tracking technique for investigation of phase recirculation and turbulence in multiphase systems. *Review of Scientific & Instruments*, *63*(10), 4361–4372.

Mudde, R.F., Groen, J.S., & van den Akker, H.E.A. (1997). Liquid field in a bubble column: LDA experiments. *Chemical Engineering Science Proceedings of the 1997 third International Conference on Gas–Liquid–Solid Reaction Engineering* (Vol. *52*(21–22), pp. 4217–4224).

Roy, S., Chen, J., Kumar, S., Al-Dahhan, M.H., & Duduković, M.P. (1997). Tomography and particle tracking studies in a liquid–solid riser. *Industrial & Engineering Chemistry Research*, *36*(11), 4666–4669.

Yang, Y.B., Devanathan, N., & Duduković, M.P. (1993). Liquid backmixing in bubble columns via computer automated radioactive particle tracking (CARPT). *Experiments in Fluids*, *16*, 1–9.

Young, M.K., Carbonell, R.G., & Ollis, D.F. (1991). Airlift bioreactors: Analysis of local-phase hydrodynamics. *The American Institute of Chemical Engineers Journal*, *37*(*3*), 403–428.